

# THE ROLE OF TIME-VARYING MERIDIONAL FLOW PATTERN DURING PAST 20 YEARS IN INFLUENCING UPCOMING SOLAR CYCLE FEATURES

M. Dikpati<sup>1</sup>, T. Corbard<sup>2</sup>, P. A. Gilman<sup>1</sup>, G. de Toma<sup>1</sup>, E. J. Rhodes<sup>3</sup>, D. A. Haber<sup>4</sup>, R. S. Bogart<sup>5</sup>, P. J. Rose<sup>3</sup>

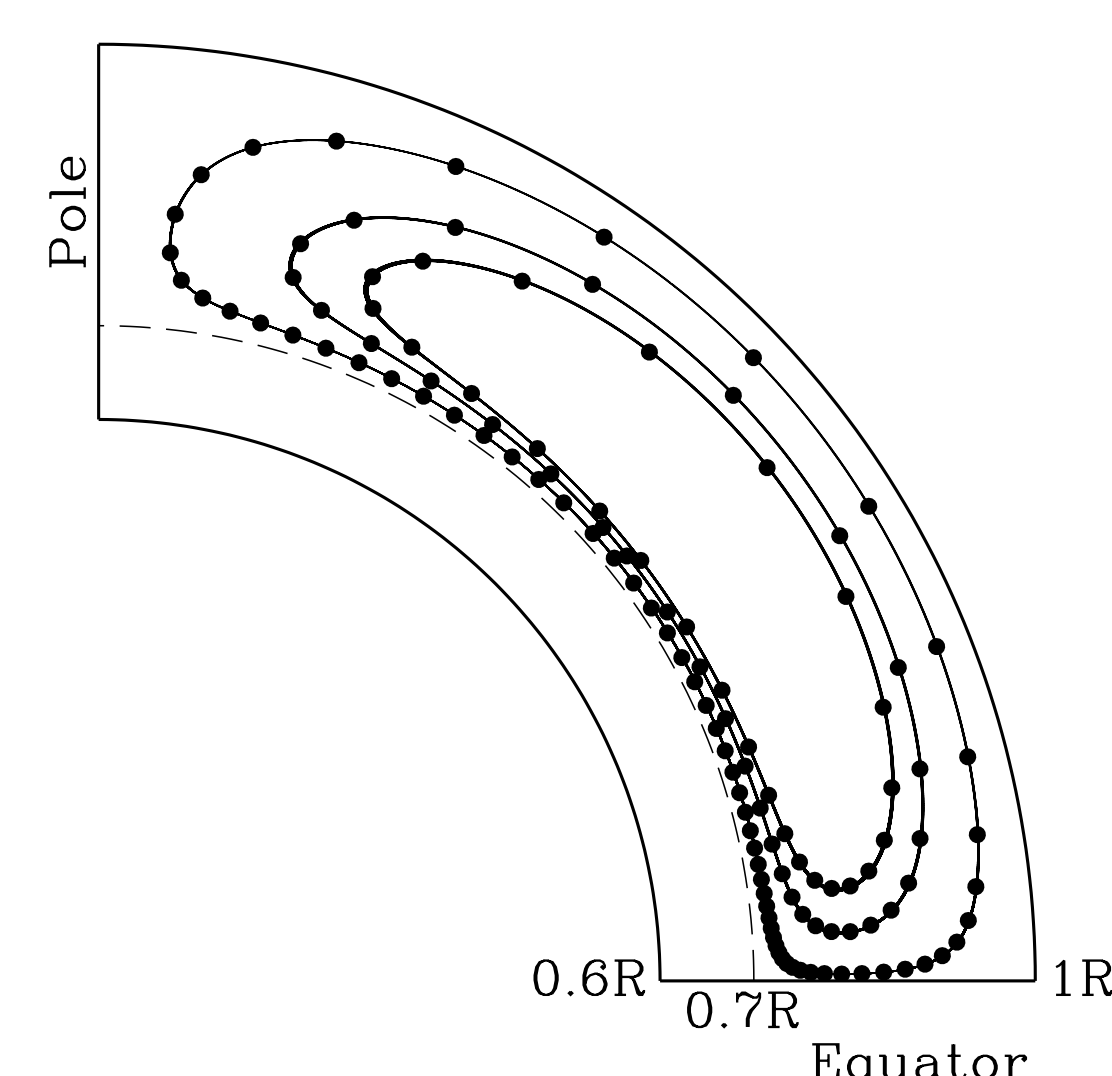
## Introduction

- Motivated by observed anomalies in cycle 23, Dikpati, de Toma, Gilman, Arge & White (2004, hereafter DDGAW) developed a flux-transport dynamo-based scheme, in order to investigate the physical cause of these anomalous features.

- These anomalies were not predicted accurately by previous schemes, primarily because those schemes used the polar field of preceding minimum ( $\sim 5.5$  years back) to determine the amplitude of the following maximum, assuming that there is correlation between these two. Schatten et al. 1978 called this correlation the “magnetic persistence”.

- DDGAW demonstrated (see Fig. 1) that the “magnetic persistence” or the Sun’s memory about its own magnetic field is governed by meridional flow speed in a flux-transport dynamo, and is longer than 5.5 years.

Fig.1: A few streamlines for the meridional circulation with solid dots plotted at time intervals of 1yr as the flow is followed along streamlines illustrate that polar fields frozen in solar plasma will be transported down to the mid-latitude of shear-layer (yellow shade) in 17-21 years. The flow is counterclockwise as observed near the surface and constructed theoretically at the base from mass conservation. It has a maximum surface flow speed of about  $15 \text{ m s}^{-1}$ . It demonstrates the physical foundation of “magnetic persistence” effect of Schatten et al. (1978).



- Fig. 1 indicates that in a flux-transport dynamo, the polar fields are advected and diffused down to the base of the convection zone in 17-21 years. They are sheared there to produce strong toroidal fields, responsible for producing spots and hence, the sunspot cycle’s strength.
- Therefore, the polar field from a few past cycles, rather than just from the preceding minima, must be taken into account in order to accurately predict the upcoming cycle’s strength.

## Polar field pattern in “peculiar” cycle 23

- Currently the information about the dynamical changes in the flow-pattern longer than 8 years into the past is not available.

- This time span is good enough for understanding the evolution of cycle 23 polar fields; so DDGAW developed a predictive tool using a flux-transport dynamo, by incorporating 8 years’ meridional flow observations (Haber et al. 2002; Basu & Antia 2002) to investigate cycle 23 polar field features (see Fig.2).

- the polar reversal was unusually slow
- the build-up of polar field after the reversal was also slow

- while N-S asymmetry in polar reversal is not unusual, and often one pole reverses after the other does, in cycle 23 the south pole reversed approximately 1 year after the north pole did.

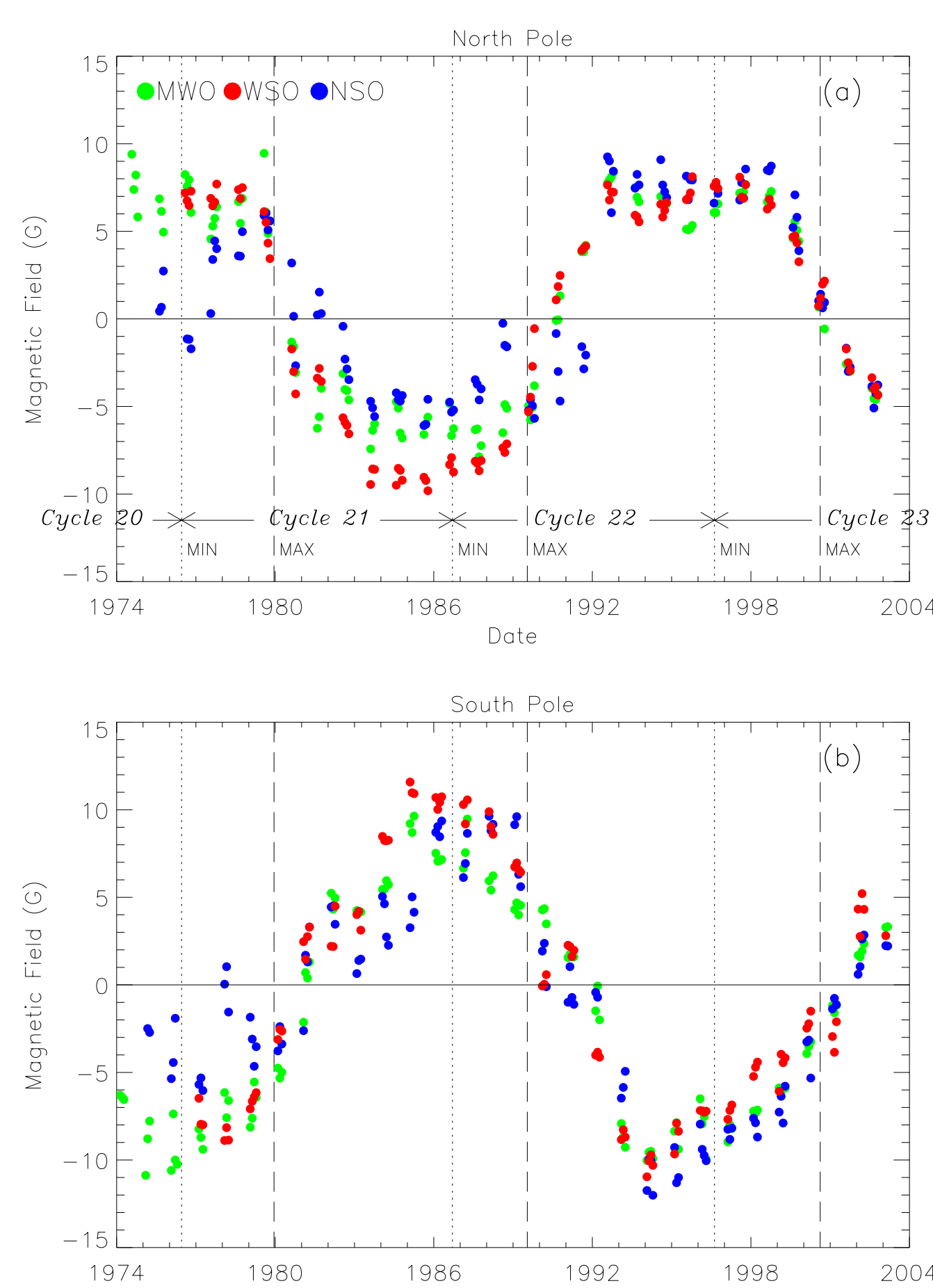


Fig.2: Average radial field strength near the pole (at  $75^\circ$ ) (a) in northern hemisphere and (b) in southern hemisphere as a function of time, plotted for each Carrington rotation since the year 1974. Measured line-of-sight fields has been adjusted to yield radial fields. Data from three different observatories, the Mount Wilson Observatory (plotted in green filled circle), the Wilcox Solar Observatory (red filled circle) and the National Solar Observatory/Kitt Peak (blue filled circle) show an overall consistency in qualitative pattern of polar fields. (Taken from Dikpati, de Toma, Gilman, Arge & White 2004.)

1. HAO/NCAR, Boulder, 3450 Mitchell Lane, CO-80301, USA  
 2. Observatoire de la Cote d’Azur, Laboratoire Cassini, B.P. 4229, F-06304 Nice, Cedex, France  
 3. Univ. of Southern California, Dept. of Physics & Astronomy, Mail Code 1342, Los Angeles, CA 90089, USA  
 4. JILA, Univ. of Colorado, Campus Box 440, Boulder, CO 80309, USA  
 5. Stanford Univ., CSSA, HEPL Annex A202, Stanford, CA 94305-4085, USA

## Calibration of Predictive Tool

DDGAW’s predictive dynamo tool operates with the following ingredients (see a schematic plot in Fig. 3):

- |   |   |
|---|---|
| (i) Differential rotation                       | → fixed by helioseismic inversion   |
| (ii) Meridional flow                            | → poleward surface flow fixed by observations (Haber et al. 2002; Basu and Antia 2002), equatorward return flow constructed from mass conservation  |
| (iii) Babcock-Leighton type surface source term | → fixed by observations of active region magnetic flux  |
| (iv) Tachocline $\alpha$ -effect                | → constructed from theoretical guidance (Ferriz-Mas, Schmitt & Schüssler 1995; Thelen 2000; Dikpati & Gilman 2001)  |
| (v) Diffusivity profile                         | → supergranular diffusivity fixed near the surface by mixing length calculations, turbulent diffusivity considered in the bulk of convection zone, $\sim$ molecular diffusivity considered at the bottom boundary in the radiative interior |
| (vi) Quenching of dynamo sources                | → parametrized following previous calculations (see Blackman & Field 2002 and references therein)   |

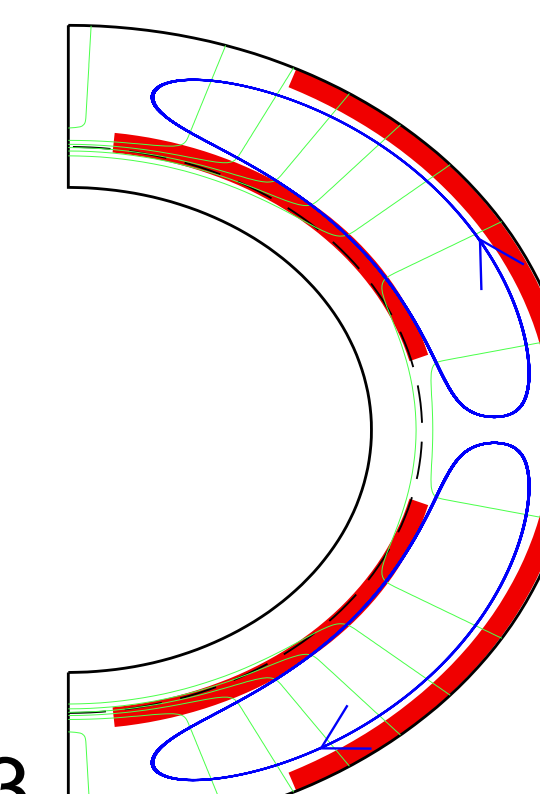


Fig. 3

DDGAW performed the validity test of calibration by comparing the map of tachocline toroidal field and surface radial field deduced from model output with the NSO map of observed longitude-averaged photospheric fields (see Fig. 4).

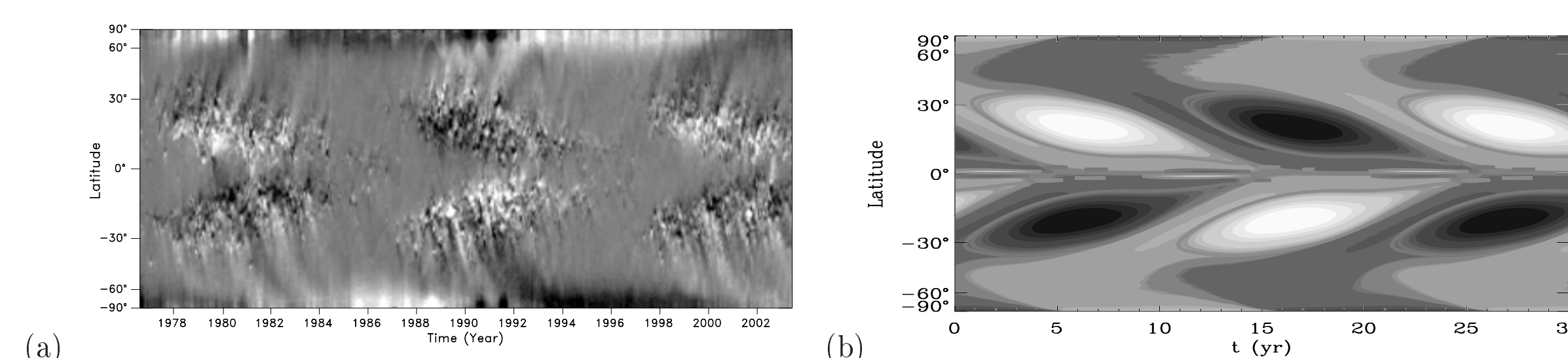


Fig.4: NSO map of observed longitude-averaged photospheric fields (left) and map of model toroidal field at convection zone base (right), from Dikpati, de Toma, Gilman, Arge & White 2004.

## Application of the tool for investigating cycle 23 polar field features

By initializing the model-scheme by solar surface magnetic field data at the beginning of the cycle 22 and operating it under the time-varying dynamo ingredients, such as time-varying surface poloidal source and meridional flow, DDGAW showed that,

- a 10-20% weakening in photospheric magnetic flux in cycle 23 with respect to that in cycle 22 is the primary reason for a  $\sim 1$  yr slowdown in polar reversal in cycle 23
- N-S asymmetry in meridional flow speed during 1996-2002 and the appearance of a reverse, high-latitude flow cell in the N-hemisphere during 1998-2001 caused the N-pole to reverse  $\sim 1$  yr before the S-pole.

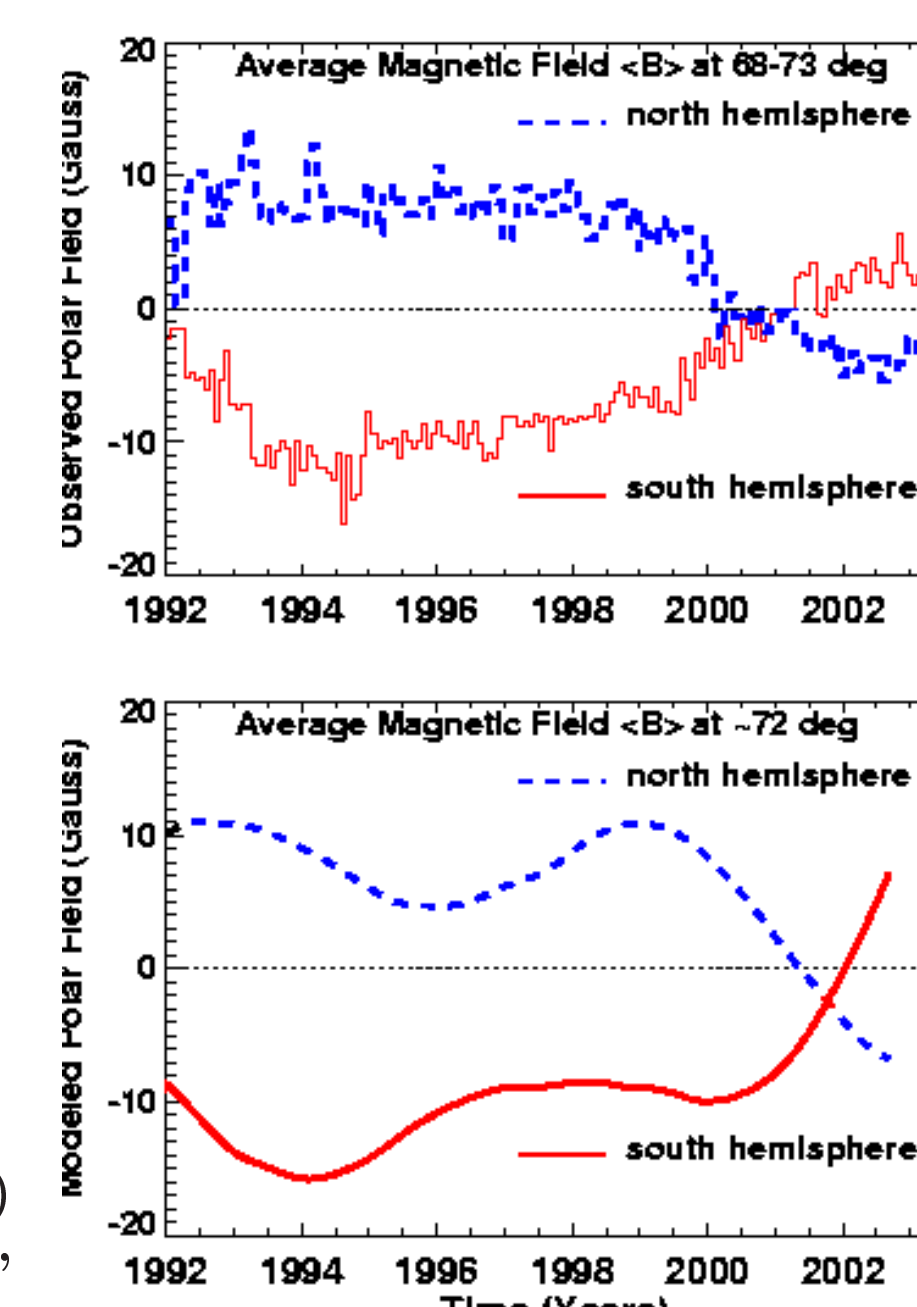


Fig.5: Observed (top) and modeled (bottom) polar fields, taken from Dikpati, de Toma, Gilman, Arge & White 2004.

## Effort on extracting 20 years’ meridional flow data

- High resolution solar Dopplergrams have been produced by MDI on board SOHO since 1996 and by the upgraded network GONG+ since 2001 which have allowed us to study the sub-photospheric meridional circulation during solar cycle 23 (Haber et al. 1998, 2000,2002; Basu et al. 2001).

- In order to extend these studies of the meridional flow over the 2 cycle period needed for our model-scheme, Rhodes et al. (2004) and Corbard et al (2004) are planing to apply the identical analysis techniques which have been applied to the MDI and GONG+ observations to a unique set of high-resolution solar Dopplergrams which have been obtained every year since 1987 at the 60-foot Solar Tower of the Mt. Wilson Observatory.

- In the pre-MDI era (i.e. prior to 1996) of MWO operations, observations were collected at MWO for a total of 1320 days, of which 649 (or 49.2%) were eight hours longer in duration and 671 days (or 50.8%) ranged up to 7.5 hours in duration. During 2003, we started to transfer this extensive archive of ground based Dopplergrams to the MDI Science Center located at Stanford University.

- A complete set of FITS keywords have also been developed, which will allow the same “ring diagram” analysis software to be employed to the MWO observations [SOI Technical Note Number 03-001, Rick Bogart & Perry Rose].

- The “ring diagram” analysis is a local helioseismology method based on the use of a plane wave approximation for a set of small areas (typically 189 overlapping areas of  $15^\circ \times 15^\circ$ ) distributed over the solar disk (Patron et al. 1995, Haber et al. 1998)

- These areas are remapped on a great circle grid and tracked at the rotation rate corresponding to their latitude.

- These data cubes are the Fourier transformed in both horizontal spatial dimensions and in time to produce a three-dimensional power spectrum of ridges corresponding to trapped acoustic waves (“ring Diagrams”).

- The ring diagrams are then fitted with a 3D power spectra model including parameters representing in the spatial wave-number directions by advection. The horizontal flow velocities at different depths within each tile are then inferred by inverting the sets of displacement parameters (Gonzales Hernandez et al. 1998, also this meeting).

- Finally, the meridional circulation is obtained as a function of depth by averging over longitude the meridional component of the inferred horizontal flows.

- The possibility of doing such analysis using MWO data has been demonstrated by the pioneering work of Patron et al. (1995) on the study of the velocity fields in the convection zone, which was carried out entirely with the use of a subset of the MWO data. Tests are currently being made to compare results obtain with MDI GONG and MWO data over one (post 1996) Carrington rotation.

## A few predictive comments on upcoming cycle 24 features

- In this model-scheme, a sharp or slow rise of a cycle is respectively governed by acceleration or deceleration in meridional flow pattern.

- Our model shows that the slow-rise in cycle 23 was due to deceleration in meridional flow (as noted by Basu & Antia 2002) during the rising phase of this cycle.

- If the flow does not accelerate during the declining phase, the cycle 23 will be a longer-than-average cycle, causing delay in the onset of cycle 24.

## References

- Arge, C. N., Hildner, E., Pizzo, V. J., & Harvey, J. W. 2002, JGR, 107, No.A10, 1319  
 Basu, S., Antia, H. M. & Bogart, R. S. 2001, ESA SP-464, 183  
 Basu, S. & Antia, H. M. 2003, ApJ, 585, 553  
 Dikpati, M., de Toma, G., Gilman, P. A., Arge, C. N. & White, O. R. 2004, ApJ, 601, 1136  
 González-Hernández, I. E., Patrón, J., Bogart, R. S., & the SOI Ring Diagrams Team. 1998, ESA SP-418, 781  
 Haber, D. A., Hindman, B. W., Toomre, J., Bogart, R. S., Schou, J., & Hill, F. 1998, ESA SP-418, 791.  
 Haber, D. A., Hindman, B. W., Toomre, J., Bogart, R. S., Thompson, M. J., & Hill, F. 2000, Solar Phys., 192, 335.  
 Haber, D. A., Hindman, B. W., Toomre, J., Bogart, R. S., Larsen, R. M., & Hill, F. 2002, ApJ, 570, 855.  
 Patrón, J., Hill, F., Rhodes, E. J., Korzennik, S. G., & Cacciani, A., 1995, ApJ, 455, 746  
 Rhodes, E. J. et al. 2004, in preparation  
 Schatten, K. H., Scherrer, P. H., Svalgaard, L., & Wilcox, J. M. 1978, GRL, 5, 411

## Acknowledgments

This work has been supported by NASA grants W-10107 & W-10175 (M.D.), S-13782-G (G.d.T.), and NAG5-11920 (D.A.H.), NAG5-10917 (D.A.H.), NAG5-12491 (D.A.H.) and NSF grant ATM-0219581 (D.A.H.). NSO/Kitt Peak magnetic data used here are produced cooperatively by NSF/NOAO, NASA/GSFC and NOAA/SEL. National Center for Atmospheric Research is sponsored by National Science Foundation.